Natural fibre composites with furanic thermoset resins. Comparison between polyfurfuryl alcohol and humins from sugar conversion.

Anna Sangregorio[a,b], *Anitha Muralidhara*[b,c], *Nathanael Guigo*[a*], *Guy Marlair*[c], *Ed de Jong*[b], *Nicolas Sbirrazzuoli*[a]

[a] Université Côte d'Azur, Institut de Chimie de Nice, CNRS, UMR 7272, 06108, Nice, France

[b] Avantium Chemicals B.V., Zekeringstraat 29, 1014 BV, Amsterdam, the Netherlands

[c] Institut national de l'environnement industriel et des risques (INERIS), Parc technologique Alata, BP 2, Verneuil-en-Halatte, Picardie, France

* corresponding author: nathanael.guigo@univ-cotedazur.fr +33489150126

Abstract

Industrial humins from biorefining process of sugars were used as reactive thermoset matrix for the preparation of humins-jute fibre composites. This material was investigated and benchmarked with jute composites prepared with polyfurfurylalcohol (PFA), a well-known biobased thermosetting resin The Dynamic Mechanical Analyses (DMA) showed glass transition temperature (T_g) associated to the relaxation of the cross-linked humins' chains at 75 °C similar to the T_g of PFA. The two types of composites revealed tensile properties in the same range and both materials demonstrated very low water uptake and good dimensional stability after immersion in

liquid water. Such higher hydrophobicity compared to raw jute mat is the consequence of the good interfacial interaction of both furanic matrix with the jute fibres in agreement with SEM observations. Fire performance of materials was also investigated, demonstrating that the fire hazard of composites was not increased by the presence of furanic matrix. Interestingly, humins composites was slightly better than PFA composites for both the thermal and fire-induced toxicity threats. This study demonstrated the possibility of using industrial humins instead of PFA as a thermoset-like resin for the next generation of biobased composites.

Keywords: Biobased thermosets; Biorefinery co-products; Wettability; Fire hazard; Furanic resins

Introduction

A transition to more sustainability in composite materials implies that both matrix and reinforcement are concerned by such a vision. In this line, lignocellulosic resources offer solutions over the traditional use of petroleum-based raw materials. For instance Dehydration of C5 and C6 sugars contained in lignocellulosic biomass leadrespectively to furfural (FF) and 5-hydroxymethylfurfural (HMF)[1,2]. Furanic compounds obtained from abundant polysaccharides (i.e. cellulose and hemicellulose) can be employed for designing efficient biobased resins[3].

Furfural is today one of the most commercially-important first-generation furan derivative, produced as a wide-spread commodity at a rate of ca. 300,000 metric tons per annum by catalytic hydrolysis of biomasses issued from a variety of crops [4,5]. Most of the furfural produced worldwide is further processed into furfuryl alcohol (FA) which is key second-generation furanic compound [6]. The carbon mass fraction,

resilient chemical inertness and thermal performance have allowed the development of numerous applications for PFA resins[7]. PFA with sand gives a material which can be emploed for making foundry moulds. FA impregnation and in-situ cross-linking in wood cell wall is employedto increase significantly wood durability[8].PFA can represent a template source of carbon leading to well-controlled nanostructures [9]. PFA is also a very good biobased substitute of phenol-formaldehyde resins for which durability and mechanical performance are demanded[4,10–13]. High performance PFA nanocomposites have been produced with silica nanoparticles or silica nanoclusters leading to materials with enhanced thermal stabilities compared to the raw matrix[5,7,14]. PFA has also been employed as a key ingredient to process carbon-carbon composites[15] and glass fibers/PFA composites[16]. Recently, the combination of PFA with natural fibres is more in the spotlight as it opens the doors to the production of all green composites[10]. FA polymerization into PFA occurs first by acid-catalyzed polycondensation reactions that will form oligomers. These latter will readily cross-link together via Diels-Alder cycloaddition [3, 6] leading to branched PFA systems.

Humins is another example of furanic biomass-derived residue that can support successful development of new thermoset material. Humins started receiving more and more attention from both the academic and industrial community[11,17–21]. When either cellulose and hemicellulose are transformed into key platform molecules, heterogeneous macromolecular residues called humins can be formed [22–24]. Humins reveals a carbon-rich structure containing mainly furanic entities with a variety of pending functional groups such as hydroxyls, ketones and aldehydes. As shown in various studies [22], humins are a perfect example of a macromolecular furanic network

containing intrinsically open structures bound to the presence of aliphatic aldehydes and ketones. However, humins' chemical structure is still under debate since detailed chemical composition of humins might significantly vary with the conditions under which they are formed, as well as due to downstream bulk separation process and post-treatment methods[17,20,25]. Humins have been suggested for a wide range of applications such as potential feedstock for bio-hydrogen production and model substrate for gasification [26,27], in the preparation of catalytic nanocomposites [19] or humins-derived porous materials [18,28,29]. Quite recently, we also demonstrated that industrial humins can be employed as a matrix to prepare 100 % sustainable composites with flax fibres [30] and for the so-called 'humination' process of wood that led to more durable wood [31]. Pin et al.[11] revealed that large quantities of humins could be included in PFA to obtain a new thermosetting cross-linked system, with enhanced mechanical properties. The open structures in humins might favor the molecular mobility and the reactivity via their aliphatic carbonyls. Isolated industrial humins are resineous product and can be further polycondensed under acidic conditions leading to a glassy resin with an infinite glass transition temperature around 70 °C [17]. To our knowledge the branching reaction in humins would occur mainly through aldol condensations [22, 23, 24] and no internal cross-link via Diels-Alder cycloadditions were so-far reported for humins.

As mention above, PFA, humins and the combination of the two were shown to be very valuable solutions towards the production of natural fibres composites [10,11,30]. Recently, natural cellulosic fibres have attracted further attention as a possible choice for the replacement of glass fibres. These fibres are not only environmentally superior to the commonly used inorganic fibres but they also entail several other advantages

[10,32,33]. However, the effective use of natural fibres in composites is still scarce compared with the use of glass or synthetic fibres. One of the main reasons is the low wettability of natural fibres with the commonly used matrix. Indeed, the common petroleum-derived matrices are typically hydrophobic, showing poor interfacial adhesion with the hydrophilic natural fibres[34]. Chemical modification of the fibres is commonly used for better compatibility and thus enhancing the final properties of the composites[35]. A different approach would be to combine a hydrophilic matrix with natural fibres, opening a plethora of new possibilities involving all green composites. Indeed, the all "green" composites route looks as a very promising and quite new research line, based on the use of biobased matrices together with natural cellulosic fibres.

In the present study, we focused on the comparison between all green composites using jute fibres with two different biobased thermosetting resins: PFA and humins. This is a substantial step beyond our seminal work on humins' based composites [30] as we intend to compare herein the similarities and complementarities between the two pinpointed furanic matrix with the traditional approach consisting in investigating the thermo-mechanical properties of their respective composites. The humins matrix could be considered as a 'more heterogeneous' PFA system without the tight Diels-Alder based cross-links and with more opened structures. In addition, special emphasis on the fire hazard has been conducted which is, to our knowledge, the first time that this approach is conducted both on PFA and humins based composites. As the two resins employed herein are structurally similar these comparisons aim at qualifying the advantages and disadvantages of using humins against PFA, this latter being nowadays already largely employed as resin in several applications. Jute fibres were selected as

one of the most common biofibers used in composites. Jute contains a reasonably high proportion of cellulose (61-71%), which promotes its stiffness[36]. Therefore, this work focuses on the production of Jute/PFA and Jute/Humins composites obtained by compression moulding. The two composites were compared to highlight the variation in mechanical properties, glass transition temperature, thermal stability, and water absorption behaviour. The goal was to obtain samples with high hydrophobicity, highlighting their potential in several applications. The composites were also observed by scanning electron microscope (SEM) focusing on the morphology at the matrix / fibres interface and their adhesion. Moreover, combustible nature of all components of the studied composites may bring flammability issues in the materials developed. Although reaction to fire of biomass fibres and composites may be improved by addition of various flame-retardants[37–39], these additives may have adverse environmental and health effects if released in well-developed fire scenarios[40,41]. Therefore, the reaction to fire performance of jute mat (with and without resin impregnation), without any fire retardant additives was also roughly explored in our study by use of modern fire calorimetry, considering existing information in the matter about PFA and humins[21].

Material and Methods

2.1 Material

Humins were produced by Avantium N.V. in their pilot plant (Geleen, the Netherlands), by conversion of fructose and glucose. para-Toluenesulfonic acid monohydrate (pTSA) was used as an acid initiator for promoting humins' cross-linking. pTSA (Mw = 190.22 g/mol, T_m = 103 – 106 °C, purity > 98.5%). Furfuryl alcohol (FA)

(purity ≥ 98%) and maleic anhydride (MA) (purity ≥ 99%) were purchased from Sigma-Aldrich and were used as received. The fibres used were a jute non-woven mat with a grammage of 600 g/m^2 employed without preliminary treatment before impregnation.

2.2 Resin and composites preparation

Preparation of resins was optimized adjusted to obtain two resins with a similar viscosity for fibre impregnation. Humins resin was prepared by preheating raw industrial humins for 20 minutes at 120 °C and then slowly adding 1.5 $\%_{wt}$ of PTSA. More details on the structure and properties of raw humins can be found in Sangregorio et al. [17]. The humins/PTSA mixture was then stirred for 5 minutes at 120 °C. The resin was homogeneously spread over the jute mat and flattened between two non-adhesive films. Then, the so-called Jute/Humins composites were prepared by compression moulding. The samples were cured at 150 °C for 30 minutes. The curing time of neat humins was previously optimized to find a relatively short curing time being realistic with industrial applications and in the meantime avoiding high temperature (i.e. T > 180 °C) that could initiate thermal degradation of jute fibres. For this purpose, preliminary rheometric measurements were conducted between 120 °C and 150 °C (results not presented). At 120 °C it will take ~25 min to reach the gel point and about one hour to reach a plateau of complex viscosity indicating a complete curing of humins while at 150 °C it will take 30 minutes to reach this plateau of viscosity. The weight ratio between humins and jute was roughly 50:50 w/w.

The PFA resin was prepared with 98 $\%_{wt}$ of FA and 2 $\%_{wt}$ of MA. MA was added to FA and mixed at 80 °C for 10 minutes. The mixture was then slowly heated up at 120 °C and mixed for 20 minutes to reach a PFA resin with a viscosity similar to humins (i.e. between 10^3 and 10^4 Pa.s at 25 °C). The PFA resin was homogeneously spread over

the jute mat and flattened between two non-adhesive films. The so-called Jute/PFA composites were prepared by compression moulding. The samples were cured at 150 °C for 90 minutes. A pressure of 2 bars was used for the preparation of both samples. The weight ratio between PFA and jute was roughly 50:50.

The different time of compression moulding between jute/humins and jute/PFA are justified by the fact that it is worth comparing samples having an approximatively similar cross-linking degree. Therefore, the glass transition temperature (T_g) of the resins was chosen as an indicator of the cross-linking degree. Care was taken to obtain composites with PFA and humins having a T_g of about 75 °C.

Samples for fire behaviour tests were prepared separately. When comparing thermo-mechanical properties or swelling behavior it is important to have cured resins presenting similar transitions (for instance T_g) in order to draw conclusions on the interaction between the resins and the fibres (assuming that the thermo-mechanical properties of the resins are thus more or less similar). However, for the fire tests, it was decided to compare composites obtained from the same process i.e. subjected to the same initial thermal treatment and assuring that the matrix resins were completely cured. Therefore both Jute/PFA and Jute/Humins samples were cured for 90 minutes at 150 °C. For both composites, the weight ratio between the resin and the fibres was 60:40. It was decided to slightly increase the contribution of the resin in comparison with the 50:50 wt ratio to enhance potential differences between the two resins regarding the fire behavior.

2.3 Dynamic mechanical analysis (DMA)

Mettler-Toledo DMA-1 was employed in tensile mode and rectangular specimens obtained from composites were tested on temperature sweeps from -40 °C to 160 °C at

a heating rate of 2 °C.min^{-1}. Measurements were performed in a single frequency of 1 Hz and a displacement of 0.1 % in auto tension offset control. A preload of 0.5 N was applied.

2.4 Tensile tests

Samples of 40 x 10 x 1.2 mm (length, width, thickness) were cut from both composites. Tensile tests were conducted using a Shimadzu testing machine with a load cell of 1 kN. The operational length was set at 40 mm and arms velocity was 5 mm/min. The Young modulus, ultimate strength at break and elongation at break were calculated from the mean values obtained from six measurements.

2.5 Thermogravimetric analysis (TGA)

TGA were performed on a the 851^{e} TGA apparatus from Mettler-Toledo Inc. Samples of about 10 mg were heated from 30 °C to 800 °C at a scanning rate of 10 °C.min^{-1} under controlled air flow (50 mL.min^{-1}).

2.6 Scanning electron microscope (SEM)

The morphology of natural fibre composites after fracture was observed by scanning electron microscopy (SEM) at the Microscopy Centre of University Côte d'Azur. Observations were done with a Tescan Vega XMU SEM at an accelerating voltage of 5 kV. All samples were coated with platinum prior to observations.

2.7 Dimensional stability

Dimensional stability of Jute/PFA and Jute/Humins composites was studied. The mass and thickness of the samples was also taken before immersion in water. The samples were then let for a specific interval of time in the water. The mass and thickness were then controlled every time the sample was taken out of the water, and the water was then replaced. The samples were let in water up to 120 hours.

2.8 Fire behaviour

Reaction to fire of samples of jute mat, jute/humins composites and jute/PFA composites of 10 cm x 10 cm was examined by use of the fire propagation apparatus (FPA) [42–45], a polyvalent fire testing bench scale fire calorimeter. All experiments were conducted in well-ventilated fire conditions in a comparative mode and under an external heat flux of 35 kW m^{-2}.

Results and Discussion

3.1 Mechanical behaviour

DMA was employed to investigate the viscoelastic behaviour of the composites. The same fibres were used as reinforcement for both composite samples, thus the differences in mechanical behaviour are mostly related to the matrices themselves or the interface between the matrices and the fibres. Storage moduli (*E'*) and the damping factor (tan δ) are plotted as a function of temperature in Figure 1. *E'* represents the stiffness of the material and is proportional to the energy stored during a loading cycle. Jute/PFA composites show higher storage modulus compared with Jute/Humins composites. Despite humins and PFA having similar furanic structure, PFA is characterized by higher furan rings density and lower aliphatic linkers. PFA chains are more rigid and less likely to move, thus contributing to increasing storage modulus. The branching through Diels−Alder cycloadditions during the polymerization of FA leads to highly rigid materials with a relatively high cross-link density[46]. The cross-link density in PFA can be decreased via furan ring opening reactions when polymerization occurs in the presence of protic polar solvents. In that respect, humins' resin is a perfect example of a PFA-like resin containing a relatively high quantity of open structures due to the acid-induced ring opening reactions of HMF derivatives[22]. The variation in properties

linked to the different structures is also highlighted when studying the variation of tan δ with temperature. Tan δ represents the damping within the material and its variation is related to macroscopic physical transitions. As shown in Figure 1, a peak in tan δ curves is observed around 75 °C for both composite samples. The maximum of the tan δ peak is associated with the cooperative α-relaxation (T_α) process, generally associated with the glass transition temperature, as a first approximation. The composite preparation process conditions were specifically optimized to obtain two samples with a similar glass transition temperature (T_g), for ease of comparison. Noteworthy, significant lower time of process (30 minutes) is needed for humins to reach the same T_g as compared with PFA (90 minutes), which is of practical interest for industrial applications. As shown in Figure 1, the relaxation peak of both PFA and humins is very broad. It indicates a large distribution of relaxation times which could be associated with heterogeneity of cross-links in these furanic matrix. Indeed, in addition to their high cross-link density, both PFA and humins are known to exhibit heterogenous distribution cross-links leading to broad tan δ peaks [5, 14, 17, 30, 46]. In the glassy state, i.e. below T_g, the damping factor value is approaching 0.05 for both samples. In this range of temperatures, the polymeric chains are blocked and the deformations are mainly elastic. For temperature above the T_g, in the rubbery state, chains can easier flow and molecular motions are less restricted. Thus, energy is dissipated and damping factor increases. The maximum value of tan δ is significantly different in the case of PFA and humins composites. Jute/Humins sample shows a higher damping factor compared to Jute/PFA, indicating higher molecular motion during relaxation process. The branching structure of humins and the numerous aliphatic linkers between the furanic rings contributes to the higher flexibility of the chains, thus increasing energy dissipation through internal

frictions. On the other hand, very small amplitude in tan δ peak is observed in PFA sample, highlighting the brittle behaviour of the matrix, due to the very rigid structure which hinders chains motion.[11,13] Results are in agreement with what was previously observed for humins based composites[30] and PFA based composites[10]. Overall, the jute/humins composites demonstrate higher damping capacity on the whole temperature range compared to jute/PFA. This can be directly linked to the higher capacity of jute/humins samples to absorb and dissipate external stresses (e.g. shock). It is also worth mentioning that the relaxation behaviour of humins occurs in a much broader temperature range (i.e. between 25 °C to 150 °C) compared to PFA (i.e. between 25 °C and 120 °C).

The tensile properties obtained from tensile tests conducted on both composites are summarized in Table 1. The composites highlights comparable tensile modulus suggesting similar stress transfer between the furanic matrix and the mat. It can be noted that the strength at break is only slightly lower for jute/humins composite (8.9 MPa) compared to jute/PFA composite (11 MPa). With similar tensile modulus between the two systems, it thus lead to slightly lower elongation at break for jute/humins composites. The stress transfer between the resin and the fibres being equivalent, the lower ultimate properties would suggest that the failure of the humins matrix occurs at lower strain compared to PFA. The higher number of structural heterogeneities inherent to the humins matrix in comparison to a rather more controlled PFA structure [22, 24, 31] could explain this behavior. Nevertheless, the results show that humins can be good substitute for replacing PFA resins leading to almost comparable ultimate properties especially for application demanding low deformations.

3.2 Morphological observations

Figure 2 shows the surface of Jute/PFA and Jute/humins composites after fracture observed by Scanning Electron Microscopy (SEM). At higher magnitude (i.e. Figure 2 **d, e**, and **i, j**), it is clearly observed that the resin is homogeneously distributed over the jute fibres. Fibres are well embedded by the matrix and both humins and PFA can fill some spaces between the individual fibres suggesting a good interface between the two phases. At lower magnitude slight differences can be observed between the fracture surface of Jute/humins (images **a, b, c**) and Jute/PFA (images **f, g, h**). Those of humins composites (i.e. images **a, b** and **c**) shows more pulled out fibre bundles compared to PFA composites (images **f, g, h**). This would suggest that interfacial bonding is slightly higher in presence of PFA. However tensile tests (Table 1) showed similar modulus (i.e. directly linked to the stress transfer) between the two systems. Contrary to PFA, humins have more heterogeneous structures - associated with larger relaxation domains (Figure 1) – and thus the interfacial strength might slightly differ from one bundle to another. Such heterogeneity in interfacial properties might lead to higher possibility of fibres dislocation in humins composites. On the other hand, the fracture surface of PFA composites show less fibres with fracture or dislocation (images **f** and **g**). The fracture is very neat and homogenous and seems to be originated from the matrix. This is typical of brittle behaviour, characteristic of PFA matrix.[11]

3.3 Thermal degradation behaviour

TG scans of Jute/PFA and Jute/Humins composites and their comparison with blank jute mat are shown in Figure 3a. A zoom in the region between 35 °C and 150 °C is shown in Figure 3b. Raw jute shows a weight loss of 6 % between 35 °C and 120 °C, corresponding to the release of water moisture absorbed from the environment. Almost 2 % of mass loss is observed for the composites samples, indicating that the fibres are

well embedded by the resin and thus almost no longer exposed to environmental moisture[47]. Loss of mass is observed in Jute/Humins composite between 180 °C and 250 °C. Humins resin might still contain some residual organic volatiles compounds which are released in this range of temperature, together with condensation products from the polymerization of non-completely reacted humins[17,30]. Jute/PFA sample shows higher thermal stability compared to humins composites. The temperature corresponding to 10% of thermal degradation ($T_{10\%}$) is 213 °C for humins' composites and 290 °C for PFA composites. From the derivative TG curve (DTG) curve of raw jute (Figure 3a), it is possible to define three regions: the first and the second between 200 °C and 400 °C, with the peak of maximum rate of mass loss at 324 °C and the third between 400 °C and 550 °C, with the peak of maximum rate of mass loss at 423 °C. The first degradation region between 175 °C and 300 °C, well marked by a DTG peak, corresponds to the degradation of both hemicellulosic residues and the aromatic moieties from the lignin. This first step is then followed by the degradation of cellulose above 300 °C[48]. The last region corresponds to the carbonization of the char residue from the natural fibres. From the DTG curve of the composite samples, two regions are observed. The first region shows a peak at around 310 °C. It should correspond to the initial degradation of hemicellulose/cellulose together with the thermos-oxidative decomposition of the furanic resins. The peak is less intense for composites compared to raw jute indicating that the rate of weight loss is lower in the presence of humins and PFA resins. In the same line, the rate of carbonization is slower with the PFA and Humins. This trend has been already observed for PFA or humins based composites with cellulosic fibres[10,30].

3.4 Water absorption behaviour

The hydrophilic nature of the natural fibres could make the composites very sensitive to moisture absorption. This would raise several problems since water absorption affects the mechanical, thermal and physical properties of the final composite[49,50]. The problem is overcome when the matrix well interacts with the fibres, thus increasing the hydrophobicity of the sample. In this way, the natural fibres are protected from the external environment, and less moisture is absorbed. Water absorption behaviour was investigated for Jute/PFA and Jute/Humins composites, and compared with the raw jute mat. The percentage of water gain was calculated by mass difference of the samples before and after immersion in water, following the equation:

$$\text{Mass gain } \% = \frac{w_f - w_i}{w_i} \qquad (1)$$

Where w_i is the mass of the sample before water immersion and w_f is the mass after immersion.

The water absorption gain as a function of time is shown in Figure 4a. Jute mat increases more than 100 % of its mass only after half an hour and keeps on increasing up to 150 %. The values are strongly scattered since the mat started splitting up after 2 hours. The Jute/humins composite increases its mass by 25 % after the first half an hour, reaching saturation. Different behaviour is observed for Jute/PFA sample. No mass increase is observed for the first 8 hours. Saturation is then reached after 48 hours getting to an increase of 25 % in mass, equal to Jute/Humins composites. PFA composite is more compact, thanks to the longer compression moulding treatment. Thus, no voids are present in the composite macrostructure. In case of humins sample, the fibres might be looser, thus making it easier for water to get inside the macrostructure in a very short time. This would explain the difference at short time.

After 48 hours, water succeeds in penetrating inside the Jute/PFA structure and saturation is reached at the same mass increase as Jute/Humins composites (i.e. 25 %).

Thickness increase as a function of time after immersion in water is presented in Figure 4b. Thickness increase was calculated by measuring the thickness of the samples before and after immersion in water, following the equation:

$$\text{Thickness increase } \% = \frac{t_f - t_i}{t_i} \text{ x } 100 \qquad (2)$$

Where t_f is the thickness after immersion in water and t_i is the thickness before immersion.

Dimensional stability behaviour is very similar to what was observed for the mass increase. Jute mat thickness sharply increases after the first half an hour. The value keeps on increasing for all the time of the measurement, increasing its thickness up to 100%. Jute/Humins sample reaches saturation after half an hour, increasing thickness up to 25%. Jute/PFA sample reaches saturation after a longer time. The thickness starts slowly increasing after half an hour and gets up to 10% more after 48 hours. As explained before, it is more difficult for water to get inside the Jute/PFA macrostructure. These results indicate very good adhesion between the fibres and the matrices, confirming what observed in the SEM pictures.

3.5 Fire hazard assessment

Results of the FPA combustion tests of jute mat, jute/humins and jute/PFA composite samples are summarized in Table 1.

From Figure 5a, we observed variations in the heat release histories and overall energy release for the neat and impregnated samples. As for nearly all cellulosic materials, the shape of the curve indicated first implication of volatiles released by the materials and burning in the gas phase, progressively replaced by charring residual

combustion, when residual fixed carbon is burning [51]. The overall energy release is much lower from the neat jute sample, to be related to the limited fire load (19.1 MJ kg^{-1}) of the 12 g test sample (jute mat), whilst significant additional fire load is brought by the impregnation process (20.2MJ kg^{-1} from humins compared to 28.9 MJ kg^{-1} from PFA). From benchmarking heat release rates and cumulative energies release in jute/humins composite and jute/PFA composite, we may conclude on some fire safety advantage of humins as innovating impregnation media, as compared to more conventional PFA. A similar trend was also recently observed by the same team for other cellulosic materials treated by impregnation of the same media[31]. As compared to peak heat release rate for jute/PFA composite (979 kW m^{-2}), we observe a reduction of some 29 % in the peak HRR for jute/humins. Similarly, less energy is globally released all over the combustion process when burning humins impregnated jute fibres as compared to burning of PFA impregnated jute fibres: this is due to the fact that less additional fire load is brought for efficient jute impregnation with humins than with PFA.

The quantities of black residues left out at the end of the combustion process in jute/humins (and jute/PFA composites (respectively 9,6 g and 7,5 g) indicated the incompleteness in combustion in impregnated samples. Moreover, it was observed that the thermal stress induced during the fire scenarios did not affect the mechanical strength of the impregnated samples in the same extent as for neat jute as reflected by the figure 5b.

From the fire toxicity viewpoint, no particular issue is raised since no heteroatoms are introduced through impregnation media used for improving jute fibres-based materials under consideration. This could essentially limit the impact to the CO threat in well-

ventilated fires as for most products containing solely C, H, and O elements, whatever chemical bonds are present. Comparing the incomplete combustion product yields presented in Table 1 (CO, CH_4, total hydrocarbons (THCs) and soot) leads to the conclusion that impregnation does not induce dramatic changes in the product yields as compared to neat jute. PFA resin combined with jute fibres lead to more sooty fires than humins'. Accordingly, humin resin shows some small advantage as compared to PFA, as far as fire safety is concerned. Fire assessment of impregnated humins/jute composites would of course deserve further considerations at higher Technological readiness levels in support of such composite commercialization.

Conclusion

This study compared the properties of jute/humins composites with jute/PFA composites. PFA is already largely used as a resin in several applications, thus the comparison aims at underlining the advantages and disadvantages of using humins against PFA. Similar glass transition temperature can be obtained for a lower time of curing process when using humins as compared with PFA. This is an advantage for industrial applications because it allows shorter times and a lower energy consumptions. The storage modulus measured by DMA is slightly higher in Jute/PFA composites; however the latter is more brittle compared with humins composites. This can be explained by the short chain segments created during Diels−Alder cyclo-additions involved in FA polymerization.. The thermal stability of jute/humins composites is lower than that of jute/PFA composites, due to the humins residual condensations occuring between 200 and 250 °C and to the very high thermal stability of PFA polymers. Dimensional stability after immersion in water was also studied showing an

increase of around 25 % for the two composites (Jute/PFA and Jute/Humins), being much lower compared with raw jute mat (100 %). The rate of water uptake is also considerably reduced for the composites. A similar conclusion is drawn for thickness increase. This indicates a very good adhesion between the fibres and the matrices, leading to a high hydrophobicity thanks to the good impregnation of hydrophilic fibres within the resin. This agrees with SEM observations. Finally, fire risks were also assessed. Despite being combustible by nature, the impregnation media only slightly increases the fire load of the composite during the combustion process. However, this does not lead to easier ignitability of the composite. Toxic species released from the combustion of composites do not significantly differ from the untreated jute material. From the fire safety viewpoint, our study supports that the impregnation process does not significantly increase the fire hazard of jute material. Moreover, our results tend to show a slight advantage for humins versus PFA for both the thermal and fire-induced toxicity threats. These results indicate that humins could have a future as a substitute PFA in several applications, underling the potential of humins to be used as resin in combination with natural fibres.

Acknowledgements

The authors acknowledge the EU framework Program Horizon 2020 for financial support as in the HUGS project (ID: 675325).

References

[1] van Putten R-J, Van der Waal JC, de Jong E, Rasrendra B, Heeres HJ, de Vries JG. Hydroxymethylfurfural, A Versatile Platform Chemical Made from Renewable Resources. ChemRev 2013;113:1499–597. doi:10.1021/cr300182k.

[2] Caes BR, Teixeira RE, Knapp KG, Raines RT. Biomass to Furanics: Renewable Routes to Chemicals and Fuels. ACS Sustain Chem Eng 2015;3:2591–605. doi:10.1021/acssuschemeng.5b00473.

[3] Gandini A, Belgacem MN. Furans in polymer chemistry. Prog Polym Sci 1997;22:1203–379. doi:10.1016/S0079-6700(97)00004-X.

[4] Deka H, Mohanty A, Misra M. Renewable-resource-based green blends from poly(furfuryl alcohol) bioresin and lignin. Macromol Mater Eng 2014;299:552–9. doi:10.1002/mame.201300221.

[5] Bosq N, Guigo N, Vincent L, Sbirrazzuoli N. Thermomechanical behavior of a novel biobased poly(furfurylalcohol)/silica nanocomposite elaborated by smart functionalization of silica nanoparticles. Polym Degrad Stab 2015;118:137–46. doi:10.1016/j.polymdegradstab.2015.04.018.

[6] Gandini A. Polymers from renewable resources: A challenge for the future of macromolecular materials. Macromolecules 2008;41:9491–504. doi:10.1021/ma801735u.

[7] Bosq N, Guigo N, Persello J, Sbirrazzuoli N. Elaboration and characterization of a novel biobased poly(furfurylalcohol)/silica nanocomposite. Adv Mater Res 2013;747:657–9. doi:10.4028/www.scientific.net/AMR.747.657.

[8] Lande S, Eikenes M, Westin M, Schneider MH. Furfurylation of wood: Chemistry, properties, and commercialization. ACS Symp Ser 2008;982:337–55. doi:10.1021/bk-2008-0982.ch020.

[9] Wang H, Yao J. Use of Poly(furfuryl alcohol) in the fabrication of nanostructured carbons and nanocomposites. Ind Eng Chem Res 2006;45:6393–404. doi:10.1021/ie0602660.

[10] Deka H, Misra M, Mohanty A. Renewable resource based "all green composites" from kenaf biofiber and poly(furfuryl alcohol) bioresin. Ind Crops Prod 2013;41:94–101. doi:10.1016/j.indcrop.2012.03.037.

[11] Pin JM, Guigo N, Mija A, Vincent L, Sbirrazzuoli N, Van Der Waal JC, et al. Valorization of biorefinery side-stream products: Combination of humins with polyfurfuryl alcohol for composite elaboration. ACS Sustain Chem Eng 2014;2:2182–90. doi:10.1021/sc5003769.

[12] Guigo N, Mija A, Vincent L, Sbirrazzuoli N. Eco-friendly composite resins based on renewable biomass resources: Polyfurfuryl alcohol/lignin thermosets. Eur Polym J 2010;46:1016–23. doi:10.1016/j.eurpolymj.2010.02.010.

[13] Pin JM, Guigo N, Vincent L, Sbirrazzuoli N, Mija A. Copolymerization as a Strategy to Combine Epoxidized Linseed Oil and Furfuryl Alcohol: The Design of a Fully Bio-Based Thermoset. ChemSusChem 2015;8:4149–61. doi:10.1002/cssc.201501259.

[14] Bosq N, Guigo N, Falco G, Persello J, Sbirrazzuoli N. Impact of Silica Nanoclusters on Furfuryl Alcohol Polymerization and Molecular Mobility. J

Phys Chem C 2017;121:7485–94. doi:10.1021/acs.jpcc.6b12882.

[15] Manocha LM. The effect of heat treatment temperature on the properties of polyfurfuryl alcohol based carbon-carbon composites. Carbon N Y 1994;32:213–23.

[16] Domínguez JC, Madsen B. Development of new biomass-based furan/glass composites manufactured by the double-vacuum-bag technique. J Compos Mater 2015;49:2993–3003. doi:10.1177/0021998314559060.

[17] Sangregorio A, Guigo N, van der Waal JC, Sbirrazzuoli N. Humins from biorefineries as thermo-reactive macromolecular systems. ChemSusChem 2018;11:4246–55. doi:10.1002/cssc.201802066.

[18] Tosi P, van Klink GPM, Celzard A, Fierro V, Vincent L, de Jong E, et al. Auto-crosslinked rigid foams derived from biorefinery by-products. ChemSusChem 2018;11(16):2797–809. doi:10.1002/cssc.201800778.

[19] Filiciotto L, Balu AM, Romero AA, Rodríguez-Castellón E, van der Waal JC, Luque R. Benign-by-design preparation of humin-based iron oxide catalytic nanocomposites. Green Chem 2017;19:4423–34. doi:10.1039/C7GC01405H.

[20] Constant S, Lancefield CS, Weckhuysen BM, Bruijnincx PCA. Quantification and Classification of Carbonyls in Industrial Humins and Lignins by 19F NMR. ACS Sustain Chem Eng 2017;5:965–72. doi:10.1021/acssuschemeng.6b02292.

[21] Muralidhara A, Tosi P, Mija A, Sbirrazzuoli N, Len C, Engelen V, et al. Insights on thermal and fire hazards of humins in support of their sustainable use in advanced biorefineries. ACS Sustain Chem Eng 2018;6(12):16692–701.

doi:10.1021/acssuschemeng.8b03971.

[22] Van Zandvoort I, Wang Y, Rasrendra CB, Van Eck ERH, Bruijnincx PCA, Heeres HJ, et al. Formation, molecular structure, and morphology of humins in biomass conversion: Influence of feedstock and processing conditions. ChemSusChem 2013;6:1745–58. doi:10.1002/cssc.201300332.

[23] Patil SKR, Lund CRF. Formation and Growth of Humins via Aldol Addition and condensation during Acid Catalyzed conversion of 5-Hydroxymethylfurfural.pdf. Energy and Fuels 2011:4745–55.

[24] Tsilomelekis G, Orella MJ, Lin Z, Cheng Z, Zheng W, Nikolakis V, et al. Molecular structure, morphology and growth mechanisms and rates of 5-hydroxymethyl furfural (HMF) derived humins. Green Chem 2016;18:1983–93. doi:10.1039/C5GC01938A.

[25] Patil SKR, Heltzel J, Lund CRF. Comparison of structural features of humins formed catalytically from glucose, fructose, and 5-hydroxymethylfurfuraldehyde. Energy and Fuels 2012;26:5281–93. doi:10.1021/ef3007454.

[26] Hoang TMC, Lefferts L, Seshan K. Valorization of humin-based byproducts from biomass processing - A route to sustainable hydrogen. ChemSusChem 2013;6:1651–8. doi:10.1002/cssc.201300446.

[27] Hoang TMC, van Eck ERH, Bula WP, Gardeniers JGE, Lefferts L, Seshan K. Humin based by-products from biomass processing as a potential carbonaceous source for synthesis gas production. Green Chem 2015;17:959–72. doi:Doi 10.1039/C4gc01324g.

[28] Kang S, Fu J, Deng Z, Jiang S, Zhong G, Xu Y, et al. Valorization of biomass hydrolysis waste: Activated carbon from humins as exceptional sorbent for wastewater treatment. Sustain 2018;10:16–9. doi:10.3390/su10061795.

[29] Chernysheva D, Chus Y, Klushin V, Lastovina T, Pudova L, Smirnova N, et al. Sustainable utilization of biomass refinery wastes for accessing activated carbons and supercapacitor electrode materials. ChemSusChem 2018. doi:10.1002/cssc.201801757.

[30] Sangregorio A, Guigo N, van der Waal JC, Sbirrazzuoli N. All "green" composites comprising flax fibres and humins' resins. Compos Sci Technol 2019;171:70–7. doi:10.1016/j.compscitech.2018.12.008.

[31] Sangregorio A, Muralidhara A, Guigo N, Marlair G, Angelici C, de Jong E, et al. Humins based resin for wood modification and properties improvement. Green Chem 2020; 22: 2786 - 2798. doi: 10.1039/C9GC03620B

[32] Muneer F. Biocomposites from Natural Polymers and Fibers. Introd Pap Fac Landsc Archit Hortic Crop Prod Sci 2015;3.

[33] Ku H, Wang H, Pattarachaiyakoop N, Trada M. A review on the tensile properties of natural fiber reinforced polymer composites. Compos Part B Eng 2011;42:856–73. doi:10.1016/j.compositesb.2011.01.010.

[34] Kim JT, Netravali AN. Mechanical, thermal, and interfacial properties of green composites with ramie fiber and soy resins. J Agric Food Chem 2010;58:5400–7. doi:10.1021/jf100317y.

[35] Sain M, Suhara P, Law S, Bouilloux A. Interface modification and mechanical

properties of natural fiber-polyolefin composite products. J Reinf Plast Compos 2005;24:121–30. doi:10.1177/0731684405041717.

[36] Corrales F, Vilaseca F, Llop M, Giron J, Mutj P. Chemical modification of jute fibers for the production of green-composites. J Hazard Mater 2007;144:730–5. doi:10.1016/j.jhazmat.2007.01.103.

[37] Jeencham R, Suppakarn N, Jarukumjorn K. Effect of flame retardants on flame retardant, mechanical, and thermal properties of sisal fiber/polypropylene composites. Compos Part B Eng 2014;56:249–53. doi:10.1016/j.compositesb.2013.08.012.

[38] Sain M, Park SH, Suhara F, Law S. Flame retardant and mechanical properties of natural fibre-PP composites containing magnesium hydroxide. Polym Degrad Stab 2004;83:363–7. doi:10.1016/S0141-3910(03)00280-5.

[39] Branda F, Malucelli G, Durante M, Piccolo A, Mazzei P, Costantini A, et al. Silica treatments: A fire retardant strategy for hemp fabric/epoxy composites. Polymers (Basel) 2016;8:1–17. doi:10.3390/polym8080313.

[40] Mngomezulu ME, John MJ, Jacobs V, Luyt AS. Review on flammability of biofibres and biocomposites. Carbohydr Polym 2014;111:149–82. doi:10.1016/j.carbpol.2014.03.071.

[41] DiNenno PJ, Drysdale D, Beyler CL, Walton WD, Custer RLP, John R. Hall J, et al. SFPE Handbook of Fire Protection Engineering. 1995. doi:10.1007/978-1-4939-2565-0_9.

[42] British Standards Institution. BS ISO 12136:2011 Reaction to Fire Tests.

Measurement of Material Properties Using a Fire Propagation Apparatus; British Standards Institution, 2011; pp 1–60 n.d. doi:10.3969/j.issn.1006-8082.2011.06.013.

[43] NFPA 287 Standard Test Methods for Measurement of Flammability of Materials in Cleanrooms Using a Fire Propagation Apparatus (FPA) 2001 Edition n.d.

[44] Pretrel H, Le Saux W, Audouin L. Determination of the heat release rate of large scale hydrocarbon pool fires in ventilated compartments. Fire Saf J 2013;62:192–205. doi:10.1016/j.firesaf.2013.01.014.

[45] ASTM E2058-13a, Standard Test Methods for Measurement of Synthetic Polymer Material Flammability Using a Fire Propagation Apparatus (FPA); ASTM International, West Conshohocken, PA, 2013 n.d. doi:10.1520/E2058-13A.2.

[46] Falco G, Guigo N, Vincent L, Sbirrazzuoli N. Opening Furan for Tailoring Properties of Bio-based Poly(Furfuryl Alcohol) Thermoset. ChemSusChem 2018;11:1805–12. doi:10.1002/cssc.201800620.

[47] Monteiro SN, Calado V, Rodriguez RJS, Margem FM. Thermogravimetric stability of polymer composites reinforced with less common lignocellulosic fibers - An overview. J Mater Res Technol 2012;1:117–26. doi:10.1016/S2238-7854(12)70021-2.

[48] Costes L, Laoutid F, Brohez S, Dubois P. Bio-based flame retardants: When nature meets fire protection. Mater Sci Eng R Reports 2017;117:1–25.

doi:10.1016/j.mser.2017.04.001.

[49] Assarar M, Scida D, El Mahi A, Poilâne C, Ayad R. Influence of water ageing on mechanical properties and damage events of two reinforced composite materials: Flax-fibres and glass-fibres. Mater Des 2011;32:788–95. doi:10.1016/j.matdes.2010.07.024.

[50] Célino A, Gonçalves O, Jacquemin F, Fréour S. Qualitative and quantitative assessment of water sorption in natural fibres using ATR-FTIR spectroscopy. Carbohydr Polym 2014;101:163–70. doi:10.1016/j.carbpol.2013.09.023.

[51] Drysdale D. An Introduction to Fire Dynamics. Chichester, UK: John Wiley & Sons, Ltd; 2011. doi:10.1002/9781119975465.

Figure captions

Figure 1. Evolution of storage modulus (*E*') and damping factor for Jute/PFA and Jute/Humins composites with temperature.

Figure 2. SEM images of surface of Jute/humins (top images a, b, c, d, e) and Jute/PFA composites (bottom images f, g, h, i, j) after fracture. The length of the white bar represents the scale indicated by each bar.

Figure 3a. TG and DTG curves of Jute/PFA and Jute/Humins composites. Neat Jute is given as reference. **3b**. Zoom of TG curves of Jute/PFA and Jute/Humins composites in the low temperature region. Neat Jute is given as reference.

Figure 4a. Percentage of water gain with time for Jute/PFA and Jute/Humins composites. Raw jute mat is given as reference.

Figure 4b. Percentage of thickness increase as function of time after immersion in water for Jute/PFA and Jute/Humins composites. Raw jute mat is given as reference.

Figure 5: a) Heat Release rate (solid lines) and **b)** cumulative heat release (dash lines) profiles of jute mat, jute/humins composite and jute/PFA composite under fire conditions **c)** jute mat, jute/humins composite and jute/PFA composite before and after the FPA tests.

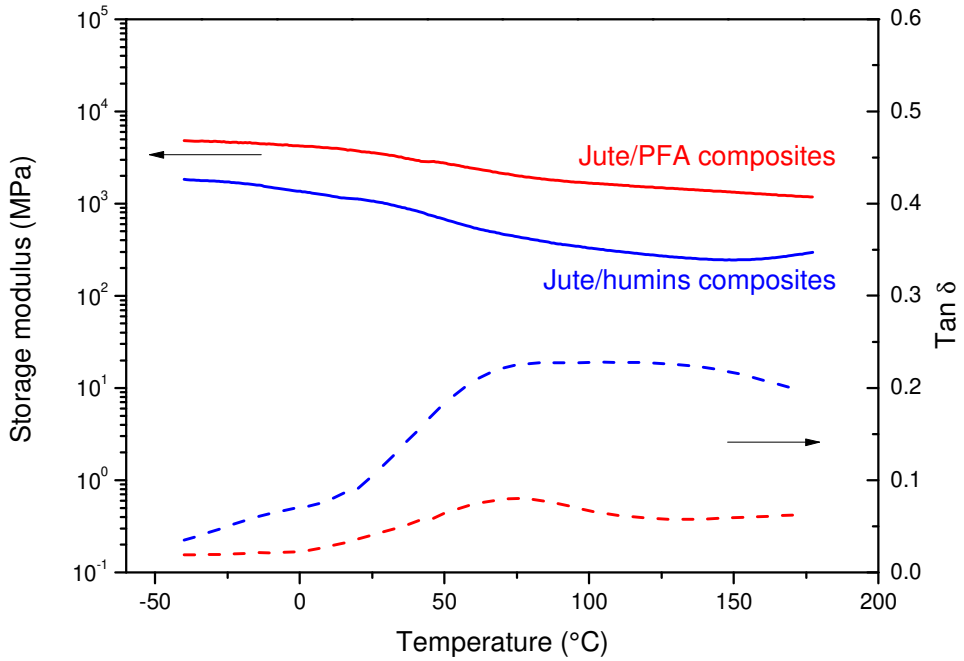

Figure 1. Evolution of storage modulus (*E*') and damping factor for Jute/PFA and Jute/Humins composites with temperature.

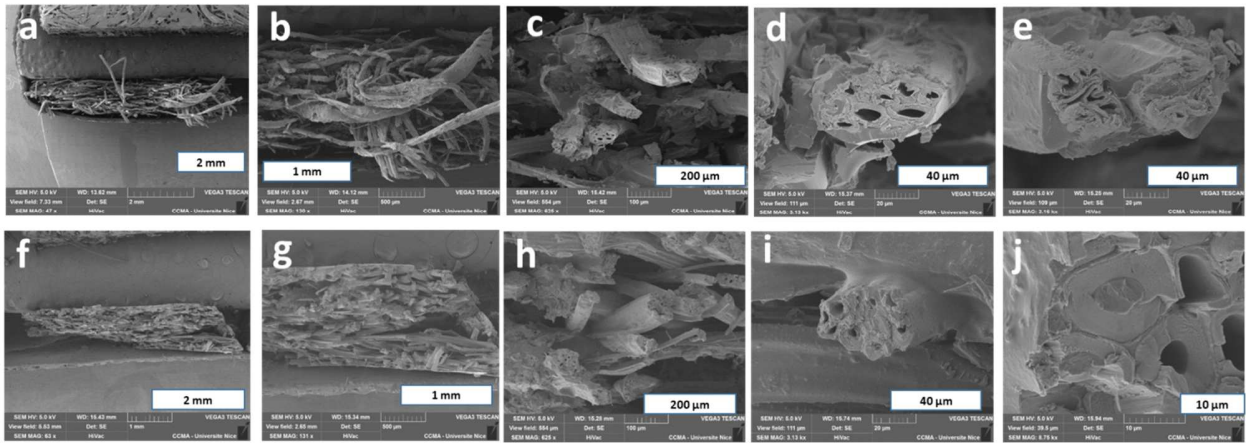

Figure 2. SEM images of surface of Jute/humins (top images a, b, c, d, e) and Jute/PFA composites (bottom images f, g, h, i, j) after fracture. The length of the white bar represents the scale indicated by each bar.

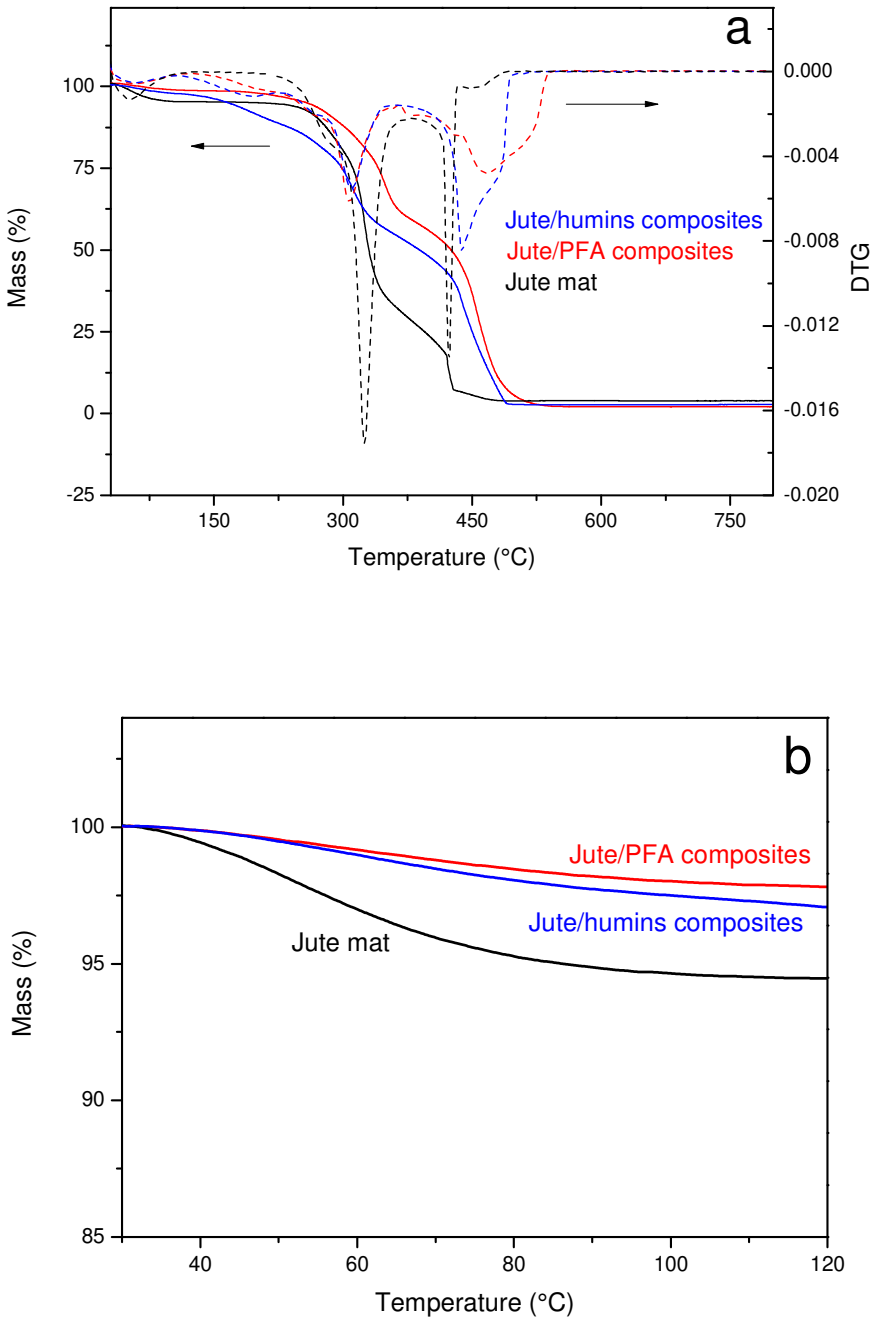

Figure 3a. TG and DTG curves of Jute/PFA and Jute/Humins composites. Neat Jute is given as reference. **3b**. Zoom of TG curves of Jute/PFA and Jute/Humins composites in the low temperature region. Neat Jute is given as reference.

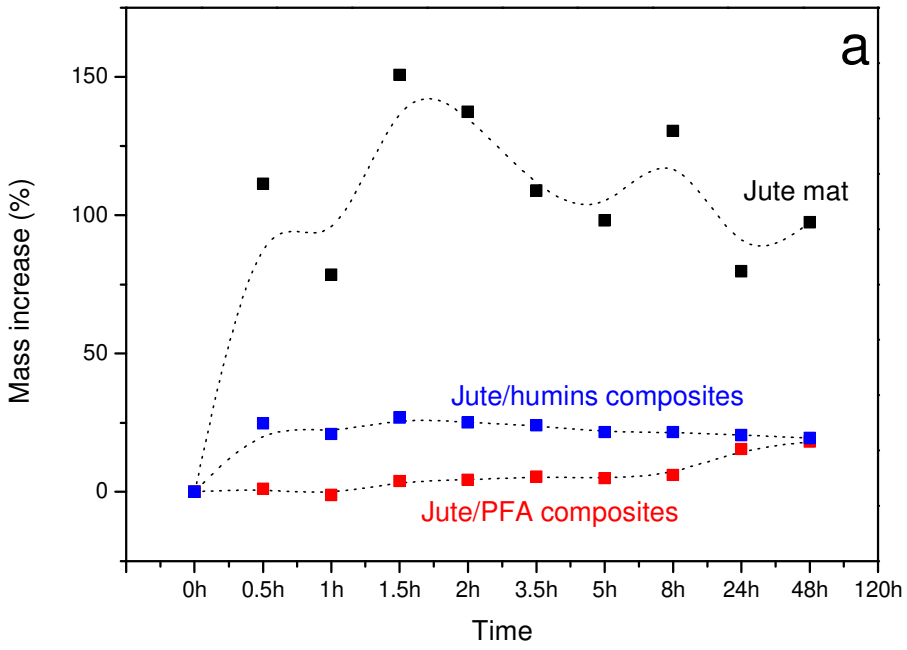

Figure 4a. Percentage of water gain with time for Jute/PFA and Jute/Humins composites. Raw jute mat is given as reference.

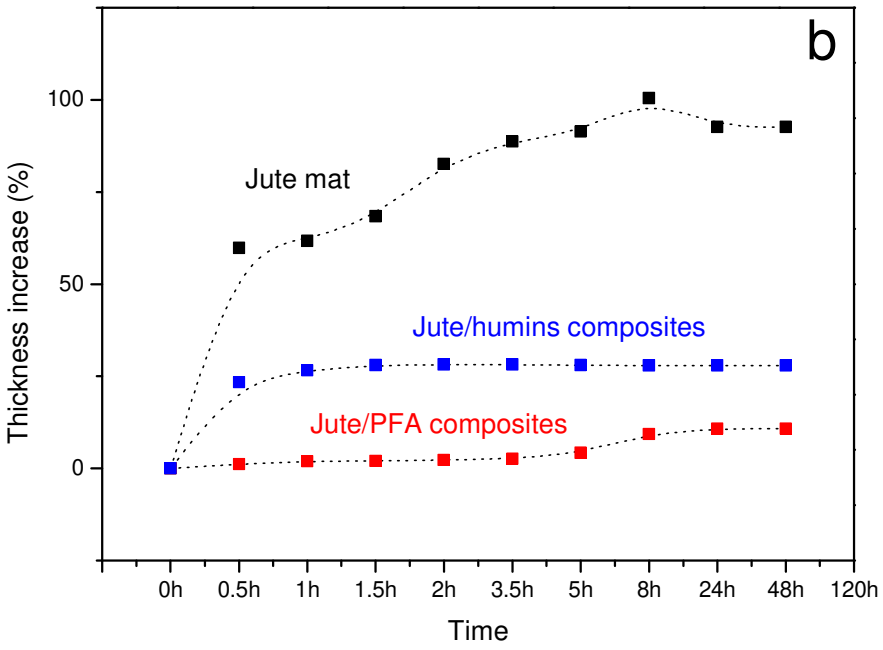

Figure 4b. Percentage of thickness increase as function of time after immersion in water for Jute/PFA and Jute/Humins composites. Raw jute mat is given as reference.

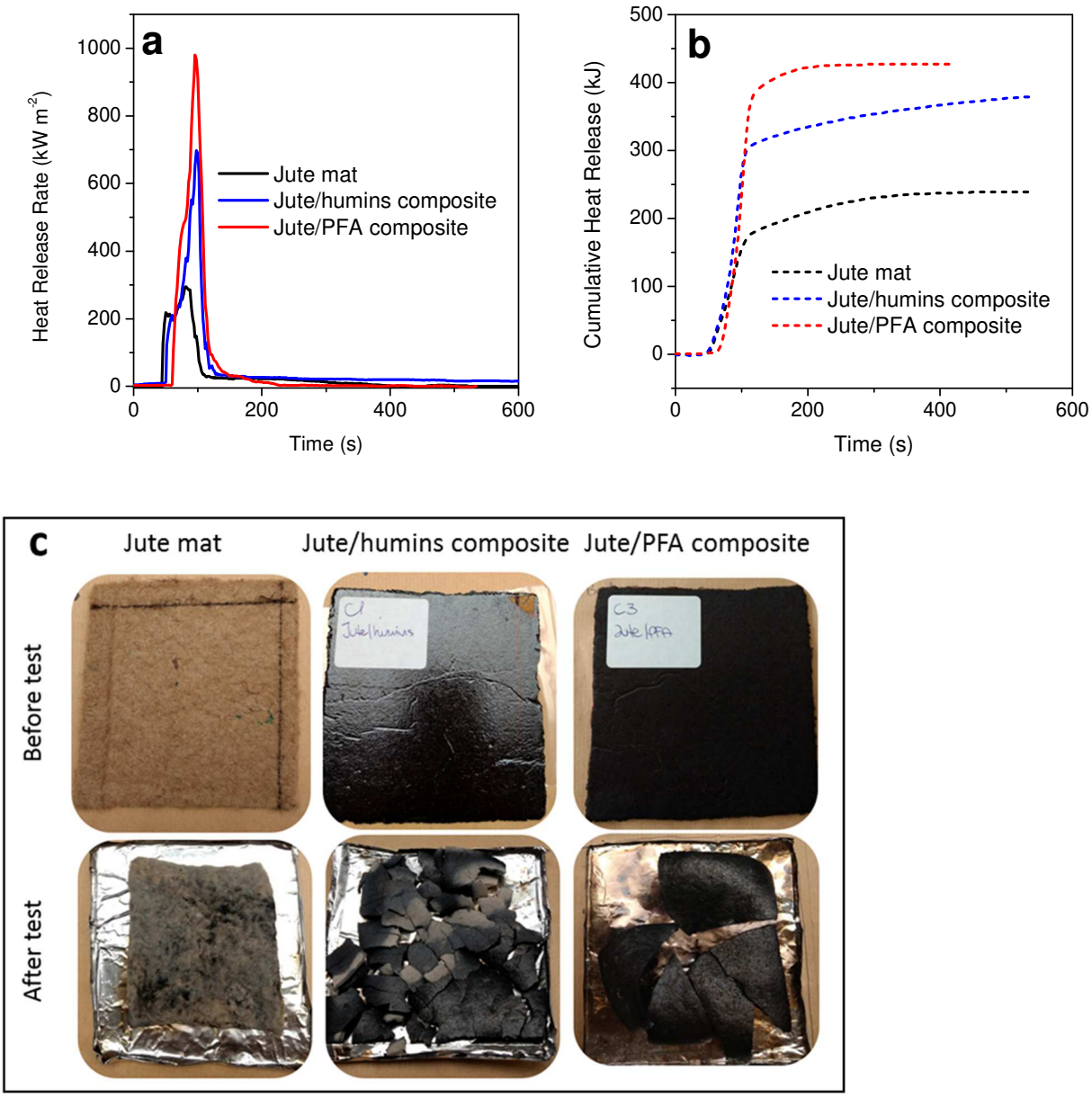

Figure 5: a) Heat Release rate (solid lines) and **b)** cumulative heat release (dash lines) profiles of jute mat, jute/humins composite and jute/PFA composite under fire conditions **c)** jute mat, jute/humins composite and jute/PFA composite before and after the FPA tests.

Table

Table 1. Tensile properties of jute/humins composites and jute/PFA composites

Measured Parameters	Tensile modulus (MPa)	Strength at break (MPa)	Elongation at break (%)
Jute/humins composite	376 ± 35	8.5 ± 0.9	3.4 ± 0.3
Jute/PFA composite	371 ± 15	11.0 ± 1.3	4.3 ± 0.7

Table 2. Burning behavior of jute mat, jute/humins composites and jute/PFA composites under well-ventilated fire conditions.

Measured Parameters	Jute mat	Jute/humins composite	Jute/PFA composite
Sample mass distribution (g)	12	16.2+15.8*=32	15.8+13.6*=29.4
Mass loss (%)	98.3	70	74.5
Time for Ignition (s)	48	53	60
Average mass loss rate (g m^{-2} s^{-1})	14.6	41.6	34.6
Max mass loss rate (g m^{-2} s^{-1})	27.4	73.2	78.7
Peak heat release rate (kW m^{-2})	294.7	698	979
Carbon mass balance (%)	85.8	86.6	97
Residue (g)	0.2	9.6	7.5
CO/CO_2	0.03	0.02	0.03
Yields of combustion products			
CO_2 (mg g^{-1})	1432	1270	1430
CO (mg g^{-1})	40	26.1	45.3
Soot (mg g^{-1})	7.8	5.2	36.5
THC (mg g^{-1})	0.6	2.7	9.1
CH_4 (mg g^{-1})	0.5	0.3	1.5

*contribution of the impregnated sample in the total sample mass.

Graphical abstract